processes

MDPI

*Article*

# Use of *Trochodendron Aralioides* Extract as Green Corrosion Inhibitor for Mild Steel in 1M HCl Solutions

**Prabu Baskar [1], Periyasamy Rathinapriya [2] and Mayakrishnan Prabakaran [3,*]**

[1] Department of Civil Engineering, Sona College of Technology, Salem 636 005, Tamil Nadu, India; prabu.civil@sonatech.ac.in
[2] Department of Biotechnology, Alagappa University, Karaikudi 630 003, Tamil Nadu, India; rathina.priya25@gmail.com
[3] Department of Crop Science, College of Sanghuh Life Science, Konkuk University, Seoul 05029, Korea
* Correspondence: prabakarannitt@gmail.com or prabakaran@konkuk.ac.kr

**Abstract:** Recently, there is an interesting discussion that has transpired around the world about the usage of plant extracts as corrosion inhibitors. We report that to control corrosion in mild steel (MS) specimens in a 1M HCl medium, *Trochodendron aralioides* (*T. aralioides*) extract was used as an economical green corrosion inhibitor. The various tests, namely, potentiodynamic polarization, weight loss measurements and electrochemical impedance spectroscopy (EIS) were performed to analyze the inhibition efficiency (IE) of the extract. The highest IE value of 96.42% was seen at 250 ppm, with the IE% increasing as the extract concentration increased. Potentiodynamic polarization suggests that *T. aralioides* plant extract acts as a mixed-type inhibitor. UV–visible (UV–Vis) and FT-IR spectroscopy were performed with the inhibitor to study the adsorption mechanism and surface analysis of the specimen, respectively. The results revealed that plant extracts form a protective film on the surface of the specimens, increasing inhibition and thereby reducing corrosion. Surface morphological studies such as AFM, EDX and SEM tests were performed in the presence and absence of the inhibitor with the results being analyzed by observing the surface of the metal.

**Keywords:** *Trochodendron aralioides*; corrosion; mild steel; electrochemical studies; adsorption; SEM-EDX; AFM



**Citation:** Baskar, P.; Rathinapriya, P.; Prabakaran, M. Use of *Trochodendron Aralioides* Extract as Green Corrosion Inhibitor for Mild Steel in 1M HCl Solutions. *Processes* **2022**, *10*, 1480. https://doi.org/10.3390/pr10081480

Academic Editor: Aneta Magdziarz

Received: 28 June 2022
Accepted: 25 July 2022
Published: 28 July 2022



## 1. Introduction

MS, also known as low carbon steel, (<0.15% of carbon) is extensively utilized in construction, fabrication and other industries due to its low cost, outstanding and easy availability, and mechanical properties such as malleability, high ductility and excellent mechanical resistance [1–3]. The major complications faced when using MS is its propensity for corrosion when exposed to aggressive media such as acidic (HCl, $H_2SO_4$), basic (NaOH, KOH) or saline atmospheres [4]. HCl is the most commonly used acid in industries for acid pickling, descaling, etc., and it is highly aggressive [3,5]. Corrosion causes deterioration of materials that leads to their destruction. It also reduces the lifespan of materials. Typically, the high cost generated by corrosion is reduced by galvanizing, applying coating or by using corrosion inhibitors. The method of using inhibitors to repress corrosion is highly effective even when added in small quantities in an extremely aggressive environment. A thin protective oxide film is created on the metal surface while using the inhibitor, which interacts with the surface physically, chemically, or a combination of both and limits cathodic and anodic reactions by hindering their active sites [6]. However, the usage of synthetic corrosion inhibitors is treacherous to the environment and uneconomical. Azoles are commonly used as synthetic corrosion inhibitors to prevent corrosion but due to the high cost, toxicity and negative impacts on the surroundings, their usage in areas such as engineering, science and technology are limited [7]. Alternatively, plant extracts are presently used as corrosion inhibitors to reduce the risk to surroundings caused by synthetic

corrosion inhibitors. Plant extracts are widely used over synthetic organic inhibitors as they are nontoxic, economical, easily available, renewable and ecofriendly [8]. The exploration for new formulations of corrosion inhibitors to prevent corrosion should satisfy new industrial needs without any threat to society. Thus, using green corrosion inhibitors has a prospective future. Various studies revealed that aqueous plant extracts can be extracted by simple techniques, leading to high efficiency as they are based on naturally occurring biodegradable organic compounds [9].

Plant extracts are recovered from various parts of plants such as roots, leaves, fruits, stems and flowers. The abundance of chemical components such as polyphenols, polysaccharides and flavonoids increase the potential of plant extracts to inhibit corrosion in MS. Natural products contain functional groups such as –CHO, -C=O and -NH2 which are viable inhibitors. On the surface of metal, these compounds are absorbed and become a defensive layer to avert corrosion. Through a survey of the literature, it was concluded that due to the existence of some complicated organic species such as proteins, tannins, alkaloids, carbohydrates and amino acids in extract, the inhibition performance of plant extract was increased [10]. Inhibitory molecules contain heterocyclic compounds with functional groups such as sulfur (S), nitrogen (N), phosphorous (P) atoms and conjugated double bonds which are major adsorption centers. The four categories of adsorption on a metal solution interface are as follows: (a) electrostatic attraction among the charged molecules and charged metal, (b) contact of metal with uncharged electron sets in the molecule, (c) interface between the metal and $\pi$ electrons and (d) association of (a) and (c) [11]. The IE of the materials while using green corrosion inhibitors depends on temperature, concentration of the extract and the corrosive media. According to the literature survey, it was found that IE when using green corrosion inhibitors was high compared to other inhibitors [12,13]. Some plant extracts used by researchers are *Azadirachta indica* [14], *Prosopis juliflora* [15], *Salvia officinalis* [16], *Dendrocalamus brandisii* [17], *Hyptis suaveolens* [18], kapok leaves extract [19], *Mangifera indica* [20], *Stachys byzantine* [21], *Glycyrrhiza glabra* [22], *Cuminum cyminum* [23], *Brassica oleracea* [24], *Ceratonia siliqua* [25], *Gongronema latifoliuim* [26], *Inula viscosa* [27], *Armoracia rusticana* [28] and *Musa paradisiaca* [29].

*T. ralioides* (wheel tree) is one of the species of the Trochodendraceae family (order Trochodendrales). It is native to the forests in Japan (Ryukyu Islands, Kyushu and Shikoku), Taiwan and Korea [30]. Its bark consists of a resinous matter known as "red bird-lime" [31]. It plays a vital part in the evolution of plants due to its primitive, less basal position. It is a unique plant as it lacks a distinguishable perianth and shows only high tepal-like scales [32]. In the wood, vessel elements are absent, which is typical of this type of angiosperm. Due to this factor, only some constituents including triterpenoids, steroids and lignans were found. The properties of Trochodendron such as growing in mild-warm temperatures, restricted elevational interludes and small intermittent populations make it difficult to envisage its sensitivity to climatic change [33]. In the secondary xylem of *T. ralioides*, being without water vessels serves as a unique feature; thus, several researchers have been curious to analyze the secondary metabolites. In the leaves of *T. ralioides*, various phytochemical components were identified [33], as shown in Figure 1. In this research, a *T. ralioides* type of green corrosion inhibitor was used on the MS specimen in 1M HCl. Tests were conducted at various concentrations to determine the IE of the plant extract, including weight loss, AAS, electrochemical measurement, FT-IR and UV–visible tests, and surface studies such as SEM, EDX and AFM studies.

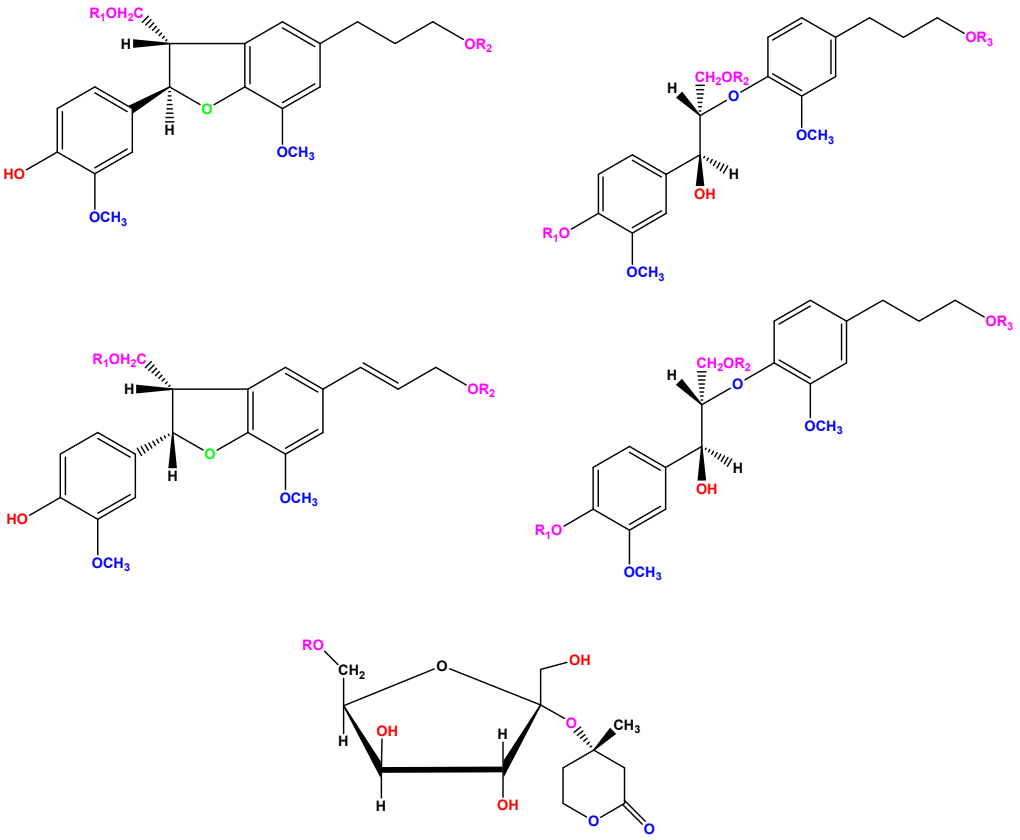


**Figure 1.** Structure of phytochemical constituents of *T. aralioides*.

## 2. Materials and Methods

### *2.1. Materials and Methods*

The chemical composition of the MS specimen comprised 0.051% carbon (C), 0.031% nickel (Ni), 0.19% manganese (Mg), 0.012% sulfur (S), 0.019% chromium (Cr), 0.018% phosphorous (P), 0.002% silicon (Si) and 0.008% molybdenum (Mo), with the remaining being iron (Fe). Methanol, HCl and acetone of AR grade were used to make 1M HCl using distilled water (triple). To measure weight loss and surface analysis, MS coupons of $3 \times 1 \times 0.5$ cm dimensions were scraped with emery sheets, degreased in acetone, dried at room temperature, and stowed in desiccators to avoid moisture captivation. Various concentrations of inhibitors ranging between 50, 100, 150, 200 and 250 ppm were added to the HCl [34].

### *2.2. Corrosion Inhibitor Preparation*

*T. aralioides* plants were acquired from Seoul, Republic of Korea. Initially, collected plants were washed with water to get rid of the presence of impurities, dried in an open atmosphere and powdered. Around 250 g of the dried fine powder was mixed with methanol and heated to the boiling point. The mixture was permitted to cool for one day and then filtered. After evaporation, pure extract was obtained. The resultant extract was used to prepare solutions of different concentrations from 50 to 250 ppm at an increment of 50 ppm by dissolving the extract in various acidic solvents [35].

### *2.3. Total Phenolic Content (TPC) and Total Flavonoid Content (TFC)*

Total phenolic content and total flavonoid content of *T. aralioides* were tested by following standard procedures [35]. Absorbance for total phenolic content was measured at 765 nm using the Optizen 2120 ultraviolet (UV) spectrometer (Mecasys, Daejeon, Korea) and the values were expressed as GAE (gallic acid equivalent) dry weight of the sample.

The absorbance for total flavonoid content was measured at 506 nm. The standard used was quercetin.

### 2.4. Techniques Used

#### 2.4.1. Weight Loss (WL) Analysis

The analysis was undertaken based upon the ASTM procedure. Weighted MS coupons were immersed in a 100 mL beaker solution containing the aggressive media 1M HCl and various concentrations in the presence and absence of *T. aralioides* (50, 100, 150, 200 and 250 ppm) for a duration of 3 h. After immersion, the steel coupons were brought out and cleaned in accordance with ASTM-31 and again weighed. The *IE*%, surface coverage ($\theta$) area and corrosion rate were calculated. The corrosion rate ($C_r$) was calculated with the help of the following Equation (1):

$$C_r = \Delta w/st \quad (1)$$

where $\Delta w$ is weight loss, $s$ is area of the specimen and $t$ is immersion time, whereas the unit of $C_r$ is mg $cm^{-2}$ $h^{-1}$. The $\theta$ and *IE*% was estimated by the subsequent Equations (2) and (3) [36]:

$$IE(\%) = \frac{(W_0 - Wi)}{(W_0)} \times 100 \quad (2)$$

$$\theta = \frac{IE(\%)}{100} \quad (3)$$

where $W_0$ and $W_i$ are the WL of the mild steel (MS) without and with the corrosion inhibitor, respectively [37].

#### 2.4.2. Electrochemical Measurements

The potentiodynamic polarization and electrochemical impedance curve were recorded with the Ivium CompactStat instrument. The test comprises three electrodes. The MS specimen was a working electrode, with the saturated calomel electrode being the reference electrode and platinum electrode being the counter electrode. The metal samples were submerged in 100 mL of 1M HCl in the presence and absence of various concentrations of the inhibitor (*T. aralioides*) at room temperature. At an open circuit potential (OCP), EIS was conducted in the frequency range and amplitude of 0.01 Hz–10 KHz and 25 mV, respectively. Tafel polarizations were performed over a potential range from −200 to +200 mV with an OCP, at a scan rate of 1 mV/s. Electrochemical parameters such as $C_{dl}$ and $R_{ct}$ were calculated using a Nyquist plot. Corrosion current density, corrosion potential, cathodic Tafel slopes and anodic potential were obtained from the experiment.

$$IE(\%) = \frac{(I'_{corr} - I_{corr})}{(I'_{corr})} \times 100 \quad (4)$$

where $I'_{corr}$ and $I_{corr}$ are the corrosion currents without and with the inhibitor. *IE* based on AC impedance was determined with the help of the following equation:

$$IE(\%) = \frac{(R_{ct} - R'_{ct})}{(R_{ct})} \times 100 \quad (5)$$

where $R_{ct}$ and $R'_{ct}$ are the corrosion currents without and with the green corrosion inhibitor [38].

### 2.5. Atomic Absorption Spectrophotometric Studies (AAS)

The instrument used to conduct AAS was the model GB 908, (Australia). The technique was to discover the quantity of iron (Fe) dissolved in the MS in the presence of corrosive

media (1M HCl) with different concentrations of extract (*T. aralioides*) for 180 min. The *IE* of the specimen tested was recorded using the following Equation (5):

$$IE\ (\%) = B - A/B \times 100 \quad (6)$$

where $B$ and $A$ are the amounts of iron dissolved in the presence and absence of the inhibitor [39].

### 2.6. FT-IR and UV–Visible Analysis

The MS coupons were immersed in hydrochloric acid of the 1M solution in the presence and absence of 250 ppm of inhibitor at a temperature of 303 ± 1 K. After 3 h, the coupons were brought out and in atmospheric temperature were dried. The surface film formed on the surface of the MS coupons was scrapped carefully and analyzed via FT-IR and UV–Vis spectroscopy. The equipment used for the analysis of FT-IR spectra and UV–Vis was the ATR-IRAffinity-1 (Shimadzu, Japan) and the LABINDIA instrument, the model UV 3000+, respectively; the results were recorded [40].

### 2.7. Surface Morphology

Scanning electron microscopy (SEM) (JEOL Model, Coimbatore, India), energy dispersive X-ray spectroscopy (EDX) (JEOL Model JSM-6390) and AFM tests were conducted for the MS coupons immersed in 1M HCl with and without *T. aralioides* extract for 3 h at 303 ± 1 K and rinsed with triple-distilled water. Subsequently, the test coupons were dried, and their morphologies observed [41].

## 3. Results and Discussion

### 3.1. TFC and TPC Analysis

The TPC of *T. aralioides* was found to be 195 mg·g$^{-1}$. TFC estimation was carried out by measuring the aluminum chloride–flavonoid complex formation. The TFC of 96 mg·g$^{-1}$ was found for *T. aralioides*. The TFC and TPC of *T. aralioides* are presented in Figure 2. The *T. aralioides* extract was identified to comprise an appreciable quantity of flavonoids and phenols which increased corrosion IE.

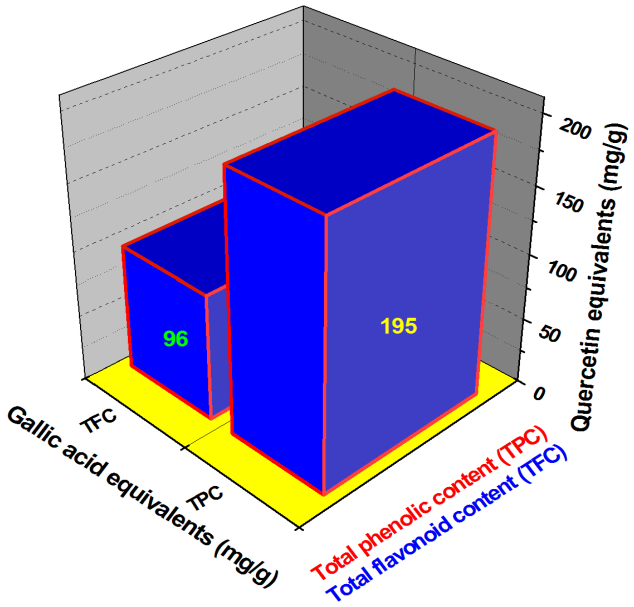


**Figure 2.** Total phenolic and flavonoid content of *T. aralioides*.

### *3.2. Weight Loss Measurements*

The measurement results of the specimens immersed in 1M HCl of several concentrations (0, 50, 100, 150, 200 and 250 ppm) of the extract (*T. aralioides*) for a duration of 180 min at atmosphere temperature are presented in Table 1.

**Table 1.** IE of T. aralioides for various concentrations against MS in 1M HCl at 303 ± 1 K by weight loss measurements.

| Conc. (ppm) | W (mg·cm$^{-2}$) | $C_r$ (mg·cm$^{-2}$ h$^{-1}$) | θ | IE% | $\sigma^a$ |
|---|---|---|---|---|---|
| Blank | 0.1231 | 0.0137 | - | - | - |
| 50 | 0.0595 | 0.0066 | 0.5166 | 51.66 | 0.05 |
| 100 | 0.0389 | 0.0043 | 0.6839 | 68.39 | 0.03 |
| 150 | 0.0256 | 0.0028 | 0.7920 | 79.20 | 0.02 |
| 200 | 0.0168 | 0.0019 | 0.8635 | 86.35 | 0.01 |
| 250 | 0.0044 | 0.0005 | 0.9642 | 96.42 | 0.01 |

$\sigma^a$ is the standard deviation.

It was noticed that the IE% increased with a rise in the quantity of plant extract at room temperature. The IE% and $C_r$ of the specimen at various amounts of the plant extract and various temperatures are presented in Table 2.

**Table 2.** IE of T. aralioides for various concentrations against MS in 1M HCl at various temperatures by WL measurement.

| T (±1 K) | Conc. (ppm) | W (mg·cm$^{-2}$) | $C_r$ (mg·cm$^{-2}$ h$^{-1}$) | θ | IE% | $\sigma^a$ |
|---|---|---|---|---|---|---|
| 313 | Blank | 0.1200 | 0.0133 | - | - | - |
| | 50 | 0.0650 | 0.0072 | 0.4583 | 45.83 | 0.04 |
| | 100 | 0.0468 | 0.0052 | 0.6100 | 61.00 | 0.06 |
| | 150 | 0.0304 | 0.0034 | 0.7466 | 74.66 | 0.01 |
| | 200 | 0.0213 | 0.0024 | 0.8075 | 80.75 | 0.05 |
| | 250 | 0.0150 | 0.0017 | 0.8750 | 87.50 | 0.01 |
| 323 | Blank | 0.1255 | 0.0139 | - | - | - |
| | 50 | 0.0751 | 0.0083 | 0.4015 | 40.15 | 0.05 |
| | 100 | 0.0535 | 0.0059 | 0.5737 | 57.37 | 0.02 |
| | 150 | 0.0393 | 0.0044 | 0.6868 | 68.68 | 0.03 |
| | 200 | 0.0285 | 0.0032 | 0.7729 | 77.29 | 0.04 |
| | 250 | 0.0210 | 0.0023 | 0.8326 | 83.26 | 0.03 |
| 333 | Blank | 0.1250 | 0.0139 | - | - | - |
| | 50 | 0.0802 | 0.0089 | 0.3584 | 35.84 | 0.01 |
| | 100 | 0.0631 | 0.0070 | 0.4952 | 49.52 | 0.03 |
| | 150 | 0.0459 | 0.0051 | 0.6328 | 63.28 | 0.02 |
| | 200 | 0.0371 | 0.0041 | 0.7032 | 70.32 | 0.01 |
| | 250 | 0.0293 | 0.0033 | 0.7656 | 76.56 | 0.04 |
| 343 | Blank | 0.1251 | 0.0139 | - | - | - |
| | 50 | 0.0901 | 0.0100 | 0.2797 | 27.97 | 0.03 |
| | 100 | 0.0711 | 0.0079 | 0.4316 | 43.16 | 0.01 |
| | 150 | 0.0533 | 0.0059 | 0.5739 | 57.39 | 0.02 |
| | 200 | 0.0484 | 0.0054 | 0.6131 | 61.31 | 0.02 |
| | 250 | 0.0400 | 0.0044 | 0.6802 | 68.02 | 0.01 |

$\sigma^a$ is the standard deviation.

There is decreased IE with increase in temperature. Increases in IE were observed with the presence of the inhibitor, reduced corrosion and enhanced surface coverage (θ). The inhibitor formed a passivation layer on the specimen and acted as an adsorbent on the metal surface [42]. An increase in temperature desorbed the barrier layer formed on the metal surface, thereby reducing surface coverage and increasing corrosion [43,44]. Maximum IE was found for the highest concentration of the plant extract (250 ppm).

### *3.3. Atomic Absorption Spectroscopy*

The AAS test was performed to analyze the dissolved ions in the corrodent solution with and without the inhibitor at various concentrations. Table 3 presents the obtained test results. The results revealed that the amount of dissolved iron decreased with the addition of a higher concentration of *T. aralioides*, protecting iron from the corrosive medium.

**Table 3.** AAS study of T. aralioides in 1M HCl with and without inhibitor at different concentrations (303 ± 1 K).

| Conc. (ppm) | Amount of MS Corrodant (mg/l) | IE% | $\sigma^a$ |
|---|---|---|---|
| Blank | 36.87 | - | - |
| 50 | 22.95 | 37.75 | 0.02 |
| 100 | 18.22 | 50.58 | 0.04 |
| 150 | 12.88 | 65.06 | 0.03 |
| 200 | 10.21 | 72.30 | 0.01 |
| 250 | 07.01 | 80.98 | 0.02 |

$\sigma^a$ is the standard deviation.

### *3.4. Electrochemical Studies*

#### 3.4.1. Potentiodynamic Polarization

Table 4 presents the electrochemical performance of the MS coupons immersed in (1M HCl) at various quantities (0, 50, 150 and 250 ppm) of the plant extract at 303 ± 1 K, which was studied using potentiodynamic polarization studies (anodic and cathodic). The increase in the concentration of extract resulted in the decreased corrosion current density ($I_{corr}$), signifying the development of a defensive coating on the MS specimen due to the inhibitor.

**Table 4.** Potentiodynamic polarization for *T. aralioides* at selected concentrations in 1M HCl at 303 ± 1 K.

| Conc. | Tafel Slopes (mV vs. dec) | | $E_{corr}$ (mV) | $I_{corr}$ ($\mu Acm^{-2}$) | IE (%) |
|---|---|---|---|---|---|
| | $b_a$ | $b_c$ | | | |
| Blank | 71 | 122 | −717.7 | 1452 | - |
| 50 | 62 | 135 | −778.0 | 464 | 68 |
| 150 | 60 | 148 | −805.5 | 327 | 77 |
| 250 | 61 | 144 | −816.8 | 188 | 87 |

A shift in corrosion potential ($E_{corr}$) was observed by comparing the polarization curves in the presence and absence of the extract. Anodic and cathodic reactions due to the green extract are shown in Figure 3. The cathodic hydrogen evolution reaction and anodic dissolution were reduced due to the addition of the plant extract, as both cathodic and anodic reactions were subsidized [45,46].

Technically, anodic polarization and cathodic polarization are the modification of anodic potential in the noble (positive) direction and the modification of cathodic potential in the active (negative) direction. The previous literature reveals that if the displacement in corrosion potential was more than 85 mV, then the inhibitor was treated either as an anodic/cathodic inhibitor, whereas if the transposition of the corrosion potential was inferior to 85 mV, then it was considered as a mixed inhibitor. Displacement of the corrosion potential of *T. aralioides* extract was found to be 99 mV, which was greater than 85 mV, indicating that the inhibitor was either cathodic or anodic [47]. IE was 87% at 250 ppm after immersion in 1M HCl for 3 h.

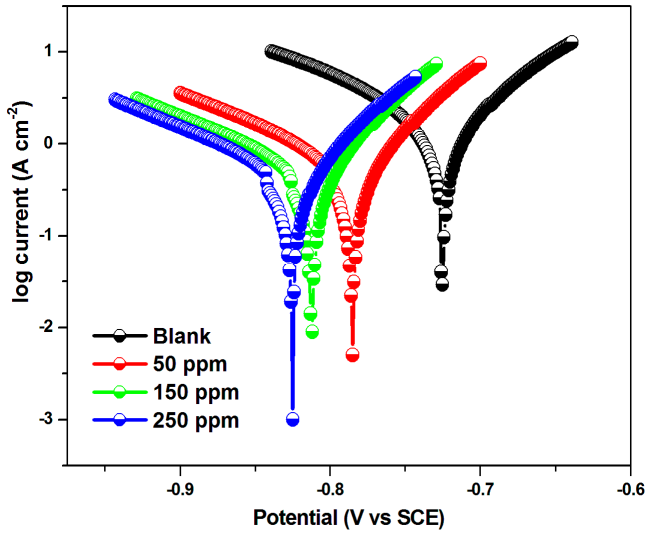


**Figure 3.** Tafel polarization plots at various concentrations of *T. aralioides*.

3.4.2. Electrochemical Impedance Spectroscopy (EIS)

This analysis was performed to understand the electrode kinetic, mechanistic and surface properties of the MS coupons in the occurrence of the corrosion inhibitor, which are illustrated in Figure 4.

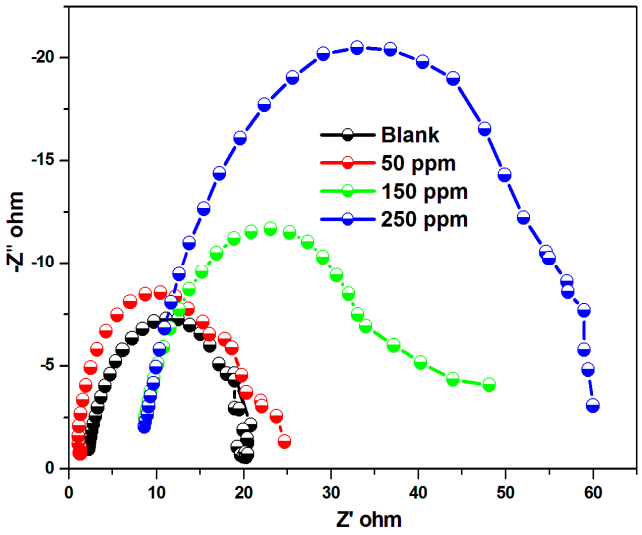


**Figure 4.** Impedance for MS specimen in 1M HCl with and without various concentrations of *T. aralioides*.

The Nyquist plot of the MS specimen immersed in 1M HCl at various concentrations is presented in Figure 4. The Nyquist plot consists of a semicircle and its center is known to have the rate of recurrence dispersion qualified to roughness and homogeneities on the surface of the metal [48]. The increase in the extract's concentration resulted in an increased diameter of the semicircle. There is significant surface coverage, and strong bonding with the surface was found with the increase in charge transfer resistance ($R_{ct}$) and the increase in the concentration of the inhibitor. The results in Table 5 indicate that the increased quantity of the inhibitor increases the charge transfer resistance and decreases the double layer capacitance due to the increased thickness of the electrical double layer.

**Table 5.** Impedance parameters for *T. aralioides* at selected concentrations in 1M HCl at 303 ± 1 K.

| Conc. | $R_{ct}$ (Ω $cm^2$) | $C_{dl}$ (Ω $cm^2$) | IE (%) |
|---|---|---|---|
| Blank | 11.12 | 50.6 | - |
| 50 | 23.51 | 44.7 | 52 |
| 150 | 38.12 | 20.8 | 71 |
| 250 | 65.26 | 16.8 | 83 |

These results showed that the inhibitor significantly adsorbed on the specimen surface [49]. The changes in the water molecules due to the extract adsorption on the metal surface reduced the dissolution level of metal, resulting in changes to the double layer capacitance ($C_{dl}$) and charge transfer resistance ($R_{ct}$) [50,51] values. A Bode plot and phase diagram of the MS specimen submerged in 1M HCl with and without the inhibitor (*T. aralioides*) at varying concentrations (0, 50, 150 and 250 ppm) at 303 ± 1 K is presented in Figure 5.

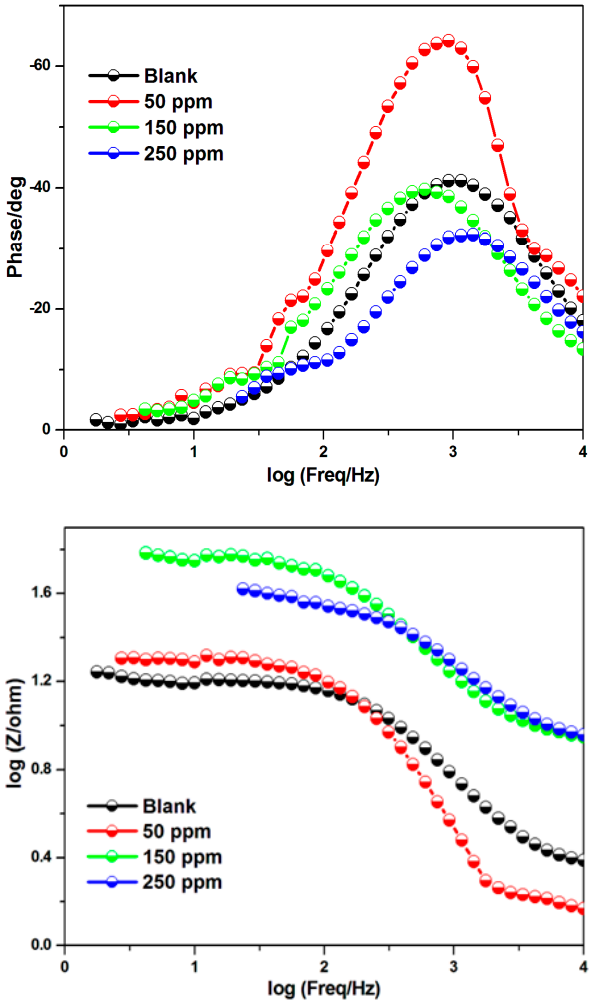


**Figure 5.** Bode and phase plot diagrams for the MS specimen in 1M HCl in various concentrations of *T. aralioides*.

It is evident from the plot that there is an increase in the phase angle shift with an increase in the concentration of the inhibitor. Polarization resistance was equal to the variance among the low-frequency limit and high-frequency limit (HF). The capacitive behavior decreased with an increase in the phase angle shift, resulting in a decrease in the metal dissolution rate. Figure 6 represents the changes in the equivalent circuit, where $C_{dl}$ is the double layer capacitance, $R_s$ is the solution resistance and $R_{ct}$ is the charge transfer resistance. The IE of the extract was found from the $R_{ct}$ data.

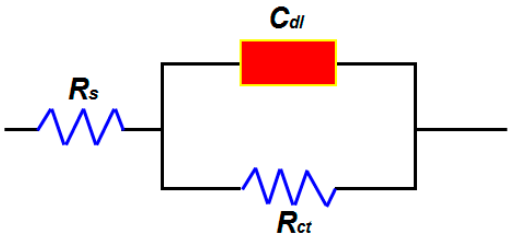


**Figure 6.** Equivalent circuit model.

### *3.5. UV–Visible Spectroscopic Analysis*

UV–Vis spectroscopy is useful to ascertain the nature of compounds present in the extract [52]. The UV–Vis analysis indicates variations in the location of the absorbance and a difference in the greater absorbance value in the presence and absence of the extract at 250 ppm submerged in 1M HCl solution, while also indicating its complex formation. The obtained spectra are shown in Figure 7.

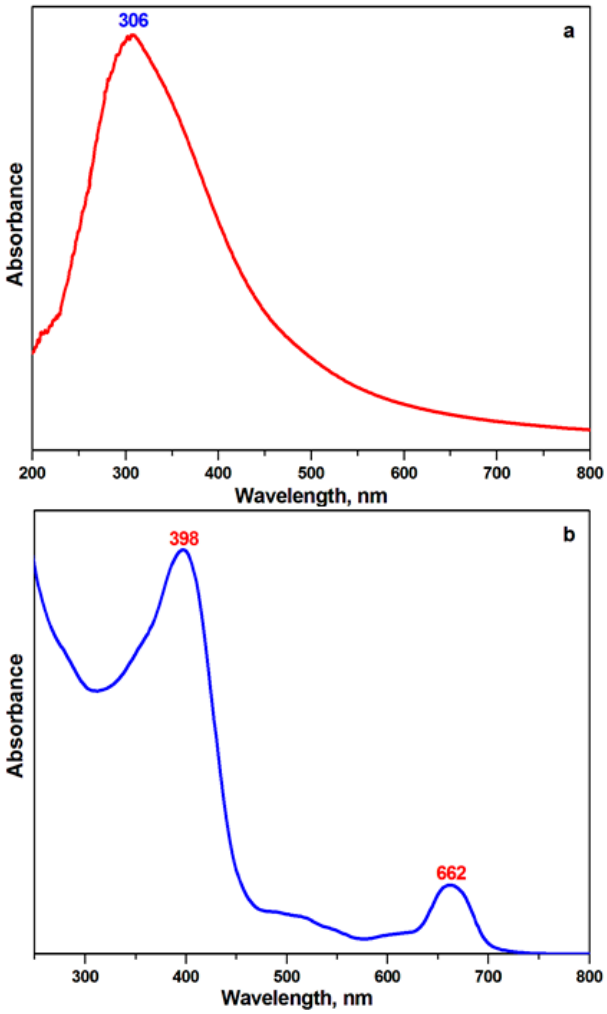


**Figure 7.** UV–visible spectra in (**a**) absence and (**b**) presence of *T. aralioides*.

The transition in the uninhibited specimen was observed at 306 nm and the transition in the inhibited specimen at 398 and 662 nm, proving that the inhibitor formed as a thin layer on the surface of the metal due to the heteroatom of the functional groups in the plant extract (*T. aralioides*), which contributed electrons to the vacant d-orbital on the metal that formed coordinate bonds and donated $\pi$-electrons to this interaction [53].

### *3.6. Fourier Transform-Infrared Spectroscopic Analysis*

FT-IR spectroscopy measures the defensive film formation on the surface and classifies the type of compound absorbed [54]. The FT-IR spectra of the raw plant extract and scrapped specimen are illustrated in Figure 8.

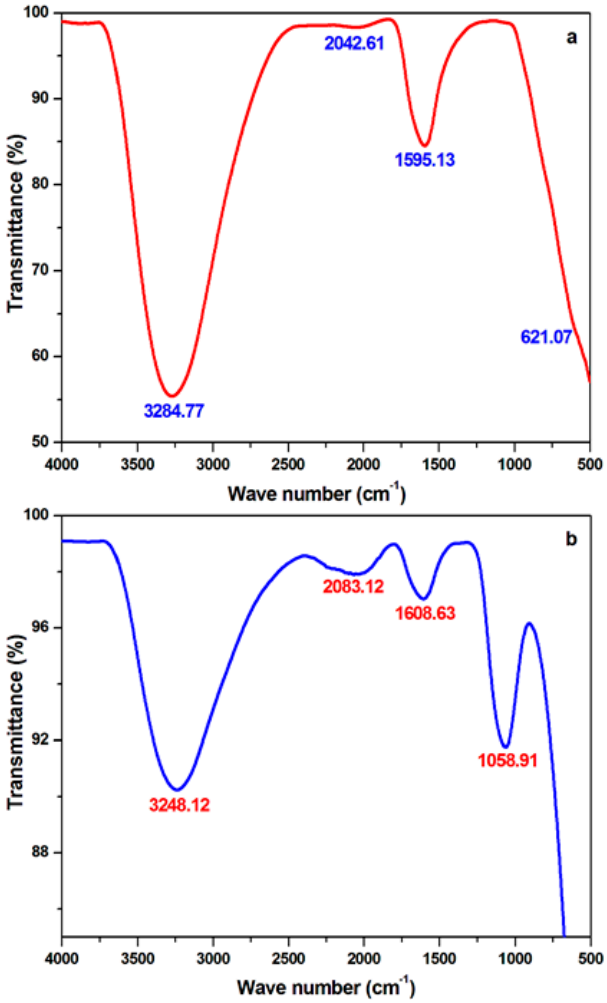


**Figure 8.** FT-IR spectrum of (**a**) *T. aralioides* corrosion inhibitor and (**b**) scrapped specimen.

The strong peak was seen at 3284.77 $cm^{-1}$ corresponding to the -OH stretching vibration. The band for -C=C-, -C=O and -C-H stretching was observed at 1595.13 $cm^{-1}$, 2042.61 $cm^{-1}$ and 621.07 $cm^{-1}$, respectively. The FT-IR spectrum of the scrapped specimen displayed a stretching frequency at 3248.12 $cm^{-1}$, 2083.12 $cm^{-1}$, 1608.63 $cm^{-1}$ and 1058.91 $cm^{-1}$, which are the performance of -OH, -C=O, -C=C- and -C-O-C- stretching vibrations, respectively. The shifts in stretching frequencies indicated that the inhibitor physically or chemically interacted on the surface of the metal. As per FT-IR data, the heteroatom of phytochemical constituents present in the inhibitor acted as a Lewis base and formed a protective layer on the metal's surface preventing corrosion [55–60].

### *3.7. Surface Analysis*

#### 3.7.1. SEM and EDX

SEM analysis was carried out to examine variations on the metal's surface in the occurrence of the presence and absence of the inhibitor. SEM analysis was conducted on the MS specimen submerged in 1M HCl with and without inhibitors at the highest concentration of 500 ppm for three hours. Figure 9a illustrates the surface morphology of the specimen in the absence of the inhibitor. The appearance of the surface was irregular

and rough due to high corrosion. Figure 9b shows the MS specimen's surface morphology in the presence of the inhibitor where a smooth surface was detected. The SEM image indicates that IE was increased by adsorption of the inhibitor on the metal's surface [61–64].

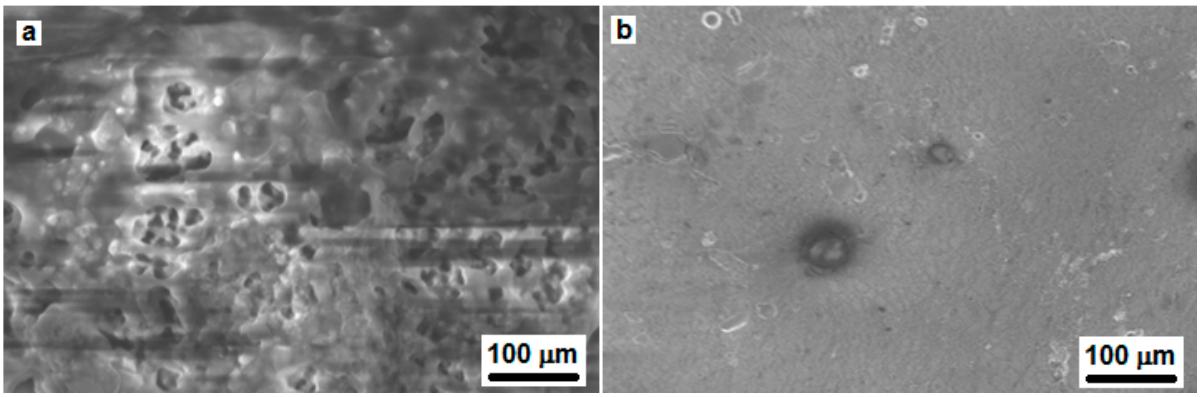


**Figure 9.** SEM images of MS: (**a**) absence of inhibitor and (**b**) presence of *T. aralioides* inhibitor extract.

EDX was implemented to discover the elements in the MS coupons that were in contact with the aggressive solution (1M HCl) in the presence and absence of the inhibitor. Table 6 exemplifies the test results.

**Table 6.** Elemental composition of the MS specimen in the absence and presence of inhibitor.

| Elements | Absence of Inhibitor (wt%) | Presence of Inhibitor (wt%) |
|---|---|---|
| C | 1.320 | 1.680 |
| O | 15.59 | 10.25 |
| Mg | 0.550 | 0.750 |
| Fe | 82.54 | 87.32 |

The EDX spectrum showed the composition of MS to be iron (Fe), 82.54%; carbon (C), 1.32%; oxygen (O), 15.59%; and magnesium (Mg), 0.55% in the absence of the inhibitor, whereas its composition in the presence of the inhibitor included iron (Fe), 87.32%; carbon (C), 1.68%; oxygen (O), 10.25%; and magnesium (Mg), 0.75% for the extract's concentration of 250 ppm. Interpreting the results revealed that after immersion for a duration of 3 h (presence of inhibitor), both oxygen and magnesium content was significantly reduced compared to in the absence of the inhibitor. The reduction in oxygen content shows a development of a protective layer on the metal's surface due to the presence of active compounds in the *T. aralioides* extract (250 ppm) as a corrosion inhibitor [65–67].

### 3.7.2. Atomic Force Microscopy

Atomic force microscopy is a dynamic tool to analyze the morphology of the surface at micro and macro levels and to examine the position of the thin film formation on the metal's surface. Figure 10 portrays the 3D AFM topography of the surface of the metal in the absence (Figure 10a) and presence (Figure 10b) of the inhibitor. The average roughness of MS exposed to the inhibitor-free 1M HCl is 278 nm and that exposed to inhibited acid is 103 nm. The reduction of average roughness indicates that the adsorbed wrapping zonal film of inhibitor molecules protects the metal from the direct attack of corrosive acid and, hence, prevents corrosion [68–72].

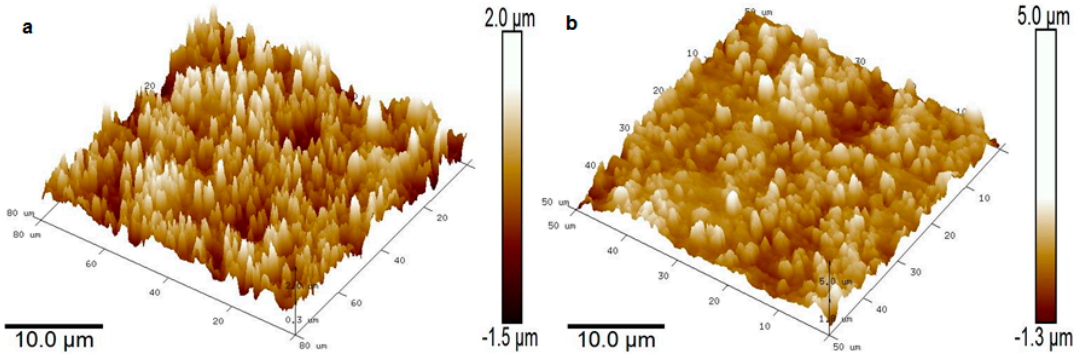


**Figure 10.** AFM 3D images of MS specimen: (**a**) without corrosion inhibitor and (**b**) with corrosion inhibitor.

## 4. Conclusions

The extract of *T. aralioides* as a green corrosion inhibitor provided effective results and demonstrated that it was an anti-corrosive inhibitor for MS in 1M HCl. WL measurements revealed that IE increased with an increase in the concentration of the extract and decreased corrosion. An increase in temperature decreased surface coverage and IE. Maximum IE was found to be 96.42% of the MS specimen exposed to 1M HCl at a concentration of 250 ppm. Tafel polarization suggests that *T. aralioides* extract acts as a mixed-type inhibitor. EIS studies specified that corrosion inhibition occurs due to the adsorption process. Spectroscopic studies such as FT-IR and UV–Vis revealed the complex formation responsible for inhibition. Surface morphological studies such as AFM, SEM and EDX substantiated the development of a thin film on the surface of the metal, which ensured protection from corrosion and increased the inhibitor's IE.

**Author Contributions:** P.B.: software, investigation, formal analysis, resources, writing—original draft, and visualization; P.R.: methodology, resources, data curation, methodology, resources, and data curation; M.P.: investigation, resources, data curation, writing—original draft, writing—review and editing, supervision, project administration, and funding acquisition. All authors have read and agreed to the published version of the manuscript.

**Funding:** This research received no external funding.

**Institutional Review Board Statement:** Not applicable.

**Informed Consent Statement:** Not applicable.

**Data Availability Statement:** Not applicable.

**Acknowledgments:** This paper was supported by the KU Research Professor Program of Konkuk University.

**Conflicts of Interest:** The authors declare no conflict of interest.

## References

1. Haldhar, R.; Prasad, D.; Bhardwaj, N. Experimental and theoretical evaluation of *Acacia catechu* extract as a natural, economical and effective corrosion inhibitor for mild steel in an acidic environment. *J. Bio Tribo Corros.* **2020**, *6*, 76. [CrossRef]
2. Sedik, A.; Lerari, D.; Salci, A.; Athmani, S.; Bachari, K.; Gecibesler, I.H.; Solmaz, R. Dardagan fruit extract as eco-friendly corrosion inhibitor for mild steel in 1M HCl: Electrochemical and surface morphological studies. *J. Taiwan Inst. Chem. Eng.* **2020**, *107*, 189–200. [CrossRef]
3. Kang, L.; Shi, L.; Zeng, Q.; Liao, B.; Wang, B.; Guo, X. Melamine resin-coated lignocellulose fibers with robust superhydrophobicity for highly effective oil/water separation. *Sep. Purif. Technol.* **2021**, *279*, 119737. [CrossRef]
4. Haldhar, R.; Prasad, D.; Bhardwaj, N. Extraction and experimental studies of *Citrus aurantifolia* as an economical and green corrosion inhibitor for mild steel in acidic media. *J. Adhes. Sci. Technol.* **2019**, *33*, 1169–1183. [CrossRef]
5. Asadi, N.; Ramezanzadeh, M.; Bahlakeh, G.; Ramezanzadeh, B. Utilizing lemon balm extract as an effective green corrosion inhibitor for mild steel in 1M HCl solution: A detailed experimental, molecular dynamics, Monte Carlo and quantum mechanics study. *J. Taiwan Inst. Chem. Eng.* **2019**, *95*, 252–272. [CrossRef]
6. Shahini, M.H.; Ramezanzadeh, B.; Mohammadloo, H.E. Recent advances in biopolymers/carbohydrate polymers as effective corrosion inhibitive macro-molecules: A review study from experimental and theoretical views. *J. Mol. Liq.* **2021**, *325*, 115110. [CrossRef]

7. Bahlakeh, G.; Ramezanzadeh, B.; Dehghani, A.; Ramezanzadeh, M. Novel cost-effective and high-performance green inhibitor based on aqueous *Peganum harmala* (Esfand) seed extract for mild steel corrosion in HCl solution: Detailed experimental and electronic/atomic level computational explorations. *J. Mol. Liq.* **2019**, *283*, 174–195. [CrossRef]
8. Haldhar, R.; Prasad, D.; Saxena, A. *Myristica fragrans* extract as an eco-friendly corrosion inhibitor for mild steel in 0.5M $H_2SO_4$ solution. *J. Environ. Chem. Eng.* **2018**, *6*, 2290–2301. [CrossRef]
9. Trindade, R.S.; Santos, M.R.; Cordeiro, R.F.B.; D'Elia, E. A study of the gorse aqueous extract as a green corrosion inhibitor for mild steel in HCl aqueous solution. *Green Chem. Lett. Rev.* **2017**, *10*, 444–454. [CrossRef]
10. Saxena, A.; Prasad, D.; Haldhar, R. Investigation of Corrosion Inhibition Effect and Adsorption activities of *Achyranthes aspera* extract for mild steel in 0.5 M $H_2SO_4$. *J. Fail. Anal. Preven.* **2018**, *18*, 957–968. [CrossRef]
11. Zaferani, S.H.; Sharifi, M.; Zaarei, D.; Shishesaz, M.R. Application of eco-friendly products as corrosion inhibitors for metals in acid pickling processes—A review. *J. Env. Chem. Eng.* **2013**, *1*, 652–657. [CrossRef]
12. Hassannejad, H.; Nouri, A. Sunflower seed hull extract as a novel green corrosion inhibitor for mild steel in HCl solution. *J. Mol. Liq.* **2018**, *254*, 377–382. [CrossRef]
13. Fernandes, C.M.; Fagundes, T.S.F.; Santos, N.E.; Rocha, T.S.M.; Garrett, R.; Borges, R.M.; Muricy, G.; Valverde, A.L.; Ponzio, E.A. *Ircinia strobilina* crude extract as corrosion inhibitor for mild steel in acid medium. *J. Electrochim. Acta* **2019**, *312*, 137–148. [CrossRef]
14. Sharma, S.K.; Mudhoo, A.; Jain, G.; Sharma, J. Corrosion inhibition and adsorption properties of *Azadirachta indica* mature leaves extract as green inhibitor for mild steel in $HNO_3$. *Green Chem. Lett. Rev.* **2010**, *3*, 7–15. [CrossRef]
15. Fouda, A.S.; Awady, G.Y.E.; Behairy, W.T.E. *Prosopis juliflora* plant extract as potential corrosion inhibitor for low carbon steel in 1M HCl solution. *J. Bio Tribo Corros.* **2018**, *4*, 8. [CrossRef]
16. Soltani, N.; Tavakkoli, N.; Khayatkashani, M.; Jalali, M.R.; Mosavizade, A. Green approach to corrosion inhibition of 304 stainless steel in hydrochloric acid solution by the extract of *Salvia officinalis* leaves. *Corros. Sci.* **2012**, *62*, 122–135. [CrossRef]
17. Li, X.; Deng, S. Inhibition effect of *Dendrocalamus brandisii* leaves extract on aluminum in HCl, $H_3PO_4$ solutions. *Corros. Sci.* **2012**, *65*, 299–308. [CrossRef]
18. Muthukrishnan, P.; Jeyaprabha, B.; Prakash, P. Mild steel corrosion inhibition by aqueous extract of *Hyptis suaveolens* leaves. *Int. J. Ind. Chem.* **2014**, *5*, 5. [CrossRef]
19. Wan, S.; Zhang, T.; Chen, H.; Liao, B.; Guo, X. Kapok leaves extract and synergistic iodide as novel effective corrosion inhibitors for Q235 carbon steel in $H_2SO_4$ medium. *Ind. Crops Prod.* **2022**, *178*, 114649. [CrossRef]
20. Ramezanzadeh, M.; Bahlakeh, G.; Sanaei, Z.; Ramezanzadeh, B. Corrosion inhibition of mild steel in 1 M HCl solution by ethanolic extract of eco-friendly *Mangifera indica* (mango) leaves: Electrochemical, molecular dynamics, Monte Carlo and ab initio study. *J. Appl. Surf. Sci.* **2019**, *463*, 1058–1077. [CrossRef]
21. Shahini, M.H.; Ramezanzadeh, M.; Ramezanzadeh, B.; Bahlakeh, G. The role of ethanolic extract of *Stachys byzantina's* leaves for effective decreasing the mild-steel (MS) degradation in the acidic solution; coupled theoretical/experimental assessments. *J. Mol. Liq.* **2021**, *329*, 115571. [CrossRef]
22. Parthipan, P.; Cheng, L.; Rajasekar, A. *Glycyrrhiza glabra* extract as an eco-friendly inhibitor for microbiologically influenced corrosion of API 5LX carbon steel in oil well produced water environments. *J. Mol. Liq.* **2021**, *333*, 115952. [CrossRef]
23. Fouda, A.S.; Rashwan, S.M.; Kamel, M.M.; Haleem, E.A. Inhibitive influence of cumin (*Cuminum cyminum*) seed extract on the dissolution of Al in 2M HCl acid medium. *J. Bio. Tribo. Corros.* **2021**, *7*, 55. [CrossRef]
24. Li, H.; Qiang, Y.; Zhao, W.; Zhang, S. A green *Brassica oleracea* L extract as a novel corrosion inhibitor for Q235 steel in two typical acid media. *Collo. Surf. A Physiochem. Eng. Asp.* **2021**, *616*, 126077. [CrossRef]
25. Fouda, A.S.; Shalabi, K.; Idress, A.A. *Ceratonia siliqua* extract as a green corrosion inhibitor for copper and brass in nitric acid solutions. *Green Chem. Lett. Rev.* **2015**, *8*, 17–29. [CrossRef]
26. Aralu, C.C.; Okorie, H.O.C.; Akpomie, G.K. Inhibition and adsorption potentials of mild steel corrosion using methanol extract of *Gongronema latifoliuim*. *Appl. Water Sci.* **2021**, *11*, 22. [CrossRef]
27. Kouache, A.; Khelifa, A.; Boutoumi, H.; Moulay, S.; Feghoul, A.; Idir, B.; Aoudj, S. Experimental and theoretical studies of *Inula viscosa* extract as a novel eco-friendly corrosion inhibitor for carbon steel in 1M HCl. *J. Adhes. Sci. Technol.* **2022**, *36*, 988–1016. [CrossRef]
28. Haldhar, R.; Prasad, D.; Saxena, A. *Armoracia rusticana* as sustainable and eco-friendly corrosion inhibitor for mild steel in 0.5M sulphuric acid: Experimental and theoretical Investigations. *J. Environ. Chem. Eng.* **2018**, *6*, 5230–5238. [CrossRef]
29. Ji, G.; Anjum, S.; Sundaram, S.; Prakash, R. *Musa paradisica* peel extract as green corrosion inhibitor for mild steel in HCl solution. *Corros. Sci.* **2018**, *90*, 107–117. [CrossRef]
30. Strijk, J.S.; Hinsinger, D.D.; Zhang, F.; Cao, K. *Trochodendron aralioides* the first chromosome-level draft genome in Trochodendrales and a valuable resource for basal eudicot research. *Gigascience* **2019**, *8*, 1–9. [CrossRef] [PubMed]
31. Yagishita, K. Isolation and identification of betulin, lupeol, and β-amyrin from the Bird-lime of *Trochodendron aralioides* Siebold et Zuccarini. *Bull. Agric. Chem. Soc. Jpn.* **1957**, *21*, 77–81. [CrossRef]
32. Wu, H.C.; Su, H.J.; Hu, J.M. The identification of A-, B-, C-, and e-class mads-box genes and implications for perianth evolution in the basal eudicot *Trochodendron aralioides* (Trochodendraceae). *Int. J. Plant Sci.* **2007**, *168*, 775–799. [CrossRef]
33. Chang, C.C.; Tsai, W.T.; Chen, C.K.; Chen, C.H.; Lee, S.S. Diastereomeric identification of neolignan rhamnosides from *Trochodendron aralioides* leaves by LC-SPE-NMR and circular dichroism. *Fitoterapia* **2020**, *144*, 104455. [CrossRef] [PubMed]
34. Prabakaran, M.; Kim, S.H.; Hemapriya, V.; Chung, I.M. *Tragia plukenetii* extract as an eco-friendly inhibitor for mild steel corrosion in HCl 1M acidic medium. *Res. Chem. Intermed.* **2016**, *42*, 3703–3719. [CrossRef]

35. Manokaran, G.; Prabakaran, M. Evaluation of antioxidant and anticorrosion activities of *Ligularia fischeri* plant extract. *Chem. Sci. Eng. Res.* **2019**, *1*, 16–24. [CrossRef]
36. Mourya, P.; Banerjee, S.; Singh, M.M. Corrosion inhibition of mild steel in acidic solution by *Tagetes erecta* (Marigold flower) extract as a green inhibitor. *Corros. Sci.* **2014**, *85*, 352–363. [CrossRef]
37. Jessima, S.J.H.M.; Subhashini, S.; Arulraj, J. *Sunova spirulina* powder as an effective environmentally friendly corrosion inhibitor for mild steel in acid medium. *J. Bio Tribo Corros.* **2020**, *6*, 71. [CrossRef]
38. Kurniawan, F.; Madurani, K.A. Electrochemical and optical microscopy study of red pepper seed oil corrosion inhibition by self-assembled monolayers (SAM) on 304 SS. *Prog. Org. Coat.* **2015**, *88*, 256–262. [CrossRef]
39. Kalaiselvi, K.; Chung, I.M.; Kim, S.H.; Prabakaran, M. Corrosion resistance of mild steel in sulphuric acid solution by *Coreopsis tinctoria* extract: Electrochemical and surface studies. *Anti-Corros. Methods Mater.* **2018**, *65*, 408–416. [CrossRef]
40. Prabakaran, M.; Kim, S.H.; Hemapriya, V.; Chung, I.M. Evaluation of polyphenol composition and anti-corrosion properties of *Cryptostegia grandiflora* plant extract on mild steel in acidic medium. *J. Ind. Eng. Chem.* **2016**, *37*, 47–56. [CrossRef]
41. Prabakaran, M.; Kim, S.H.; Mugila, N.; Hemapriya, V.; Parameswari, K.; Chitra, S.; Chung, I.M. *Aster koraiensis* as nontoxic corrosion inhibitor for mild steel in sulfuric acid. *J. Ind. Eng. Chem.* **2017**, *52*, 235–242. [CrossRef]
42. El-Etre, A.Y. Inhibition of C-steel corrosion in acidic solution using the aqueous extract of zallouh root. *J. Mater. Chem. Phys.* **2008**, *108*, 278–282. [CrossRef]
43. Satapathy, A.K.; Gunasekaran, G.; Sahoo, S.C.; Amit, K.; Rodrigues, P.V. Corrosion inhibition by *Justicia gendarussa* plant extract in hydrochloric acid solution. *Corros. Sci.* **2009**, *51*, 2848–2856. [CrossRef]
44. Khadom, A.A.; Abd, A.N.; Ahmed, N.A. *Xanthium strumarium* leaves extracts as a friendly corrosion inhibitor of low carbon steel in hydrochloric acid: Kinetics and mathematical studies. *S. Afr. J. Chem. Eng.* **2018**, *25*, 13–21. [CrossRef]
45. Fouda, A.S.; Abousalem, A.S.; El-Ewady, G.Y. Mitigation of corrosion of carbon steel in acidic solutions using an aqueous extract of *Tilia cordata* as green corrosion inhibitor. *Int. J. Ind. Chem.* **2017**, *8*, 61–73. [CrossRef]
46. Alvarez, P.E.; Fiori-Bimbi, M.V.; Neske, A.; Brand'an, S.A.; Gervasi, C.A. *Rollinia occidentalis* extract as green corrosion inhibitor for carbon steel in HCl solution. *J. Ind. Eng. Chem.* **2018**, *58*, 92–99. [CrossRef]
47. Hussin, M.H.; Kassim, M.J. The corrosion inhibition and adsorption behavior of *Uncaria gambir* extract on mild steel in 1M HCl. *Mater. Chem. Phys.* **2011**, *125*, 461–468.
48. Lebrini, M.; Robert, F.; Lecante, A.; Roos, C. Corrosion inhibition of C38 steel in 1M hydrochloric acid medium by alkaloids extract from *Oxandra asbeckii* plant. *Corros. Sci.* **2011**, *53*, 687–695. [CrossRef]
49. Bammou, L.; Belkhaouda, M.; Salghi, R.; Benali, O.; Zarrouk, A.; Zarrok, H.; Hammouti, B. Corrosion inhibition of steel in sulfuric acidic solution by the *Chenopodium ambrosioides* extracts. *J. Assoc. Arab. Univ. Basic Appl. Sci.* **2014**, *16*, 83–90. [CrossRef]
50. Prabakaran, M.; Kim, S.H.; Oh, Y.T.; Raj, V.; Chung, I.M. Anticorrosion properties of momilactone A isolated from rich hulls. *J. Ind. Eng. Chem.* **2017**, *45*, 380–386. [CrossRef]
51. Jyothi, S.; Ravichandran, J. Inhibitive action of the acid extract of *Luffa aegyptiaca* leaves on the corrosion of mild steel in acidic medium. *J. Adhes. Sci. Technol.* **2015**, *29*, 207–231. [CrossRef]
52. Fouda, A.S.; Mohamed, O.A.; Elabbasy, H.M. *Ferula hermonis* plant extract as safe corrosion inhibitor for zinc in hydrochloric acid solution. *J. Bio Tribo Corros.* **2021**, *7*, 135. [CrossRef]
53. Chung, I.M.; Malathy, R.; Priyadharshini, R.; Hemapriya, V.; Kim, S.H.; Prabakaran, M. Inhibition of mild steel corrosion using *Magnolia kobus* extract in sulphuric acid medium. *Mater. Today Commun.* **2020**, *25*, 101687. [CrossRef]
54. Li, L.; Zhang, X.; Lei, J.; He, J.; Zhang, S.; Pan, F. Adsorption and corrosion inhibition of *Osmanthus fragran* leaves extract on carbon steel. *Corros. Sci.* **2012**, *63*, 82–90. [CrossRef]
55. Saxena, A.; Prasad, D.; Haldhar, R.; Singh, G.; Kumar, A. Use of *Sida cordifolia* extract as green inhibitor for mild steel in 0.5M $H_2SO_4$. *J. Environ. Chem. Eng.* **2018**, *6*, 694–700. [CrossRef]
56. Prabakaran, M.; Kim, S.H.; Kalaiselvi, K.; Hemapriya, V.; Chung, I.M. Highly efficient *Ligularia fischeri* green extract for the protection against corrosion of mild steel in acidic medium: Electrochemical and spectroscopic investigations. *J. Taiwan Inst. Chem. Eng.* **2016**, *59*, 553–562. [CrossRef]
57. Hemapriya, V.; Prabakaran, M.; Parameswari, K.; Chitra, S.; Kim, S.H.; Chung, I.M. Experimental and theoretical studies on inhibition of benzothiazines against corrosion of mild steel in acidic medium. *Anti-Corros. Methods Mater.* **2017**, *64*, 306–314. [CrossRef]
58. Chung, I.M.; Hemapriya, V.; Ponnusamy, K.; Arunadevi, N.; Chitra, S.; Chi, H.Y.; Kim, S.H.; Prabakaran, M. Assessment of low carbon steel corrosion inhibition by ecofriendly green *Chaenomeles sinensis* extract in acid medium. *J. Electrochem. Sci. Technol.* **2018**, *9*, 238–249. [CrossRef]
59. Chung, I.M.; Hemapriya, V.; Kim, S.H.; Ponnusamy, K.; Arunadevi, N.; Chitra, S.; Prabakaran, M.; Gopiraman, M. *Liriope platyphylla* extract as a green inhibitor for mild steel corrosion in sulfuric acid medium. *Chem. Eng. Commun.* **2021**, *208*, 72–88. [CrossRef]
60. Hemapriya, V.; Chung, I.M.; Kim, S.H.; Prabakaran, M. Inhibitory effect of biowaste on copper corrosion in 1 M HCl solution. *Mater. Today Commun.* **2021**, *27*, 102249. [CrossRef]
61. Zeng, Y.; Kang, L.; Wu, Y.; Wan, S.; Liao, B.; Li, N.; Guo, X. Melamine modified carbon dots as high effective corrosion inhibitor for Q235 carbon steel in neutral 3.5 wt% NaCl solution. *J. Mol. Liq.* **2022**, *349*, 118108. [CrossRef]
62. Chitra, S.; Chung, I.M.; Kim, S.H.; Prabakaran, M. A study on anticorrosive property of phenolic components from *Pachysandra terminalis* against low carbon steel corrosion in acidic medium. *Pigment. Resin Technol.* **2019**, *48*, 389–396. [CrossRef]

63. Shamsuzzaman, M.; Kalaiselvi, K.; Prabakaran, M. Evaluation of antioxidant and anticorrosive activities of *Ceriops tagal* plant extract. *Appl. Sci.* **2021**, *11*, 10150. [CrossRef]
64. Chung, I.M.; Kalaiselvi, K.; Sasireka, A.; Kim, S.H.; Prabakaran, M. Anticorrosive property of *Spiraea cantoniensisis* extract as an eco-friendly inhibitor on mild steel surface in acid medium. *J. Dispers. Sci. Technol.* **2019**, *40*, 1326–1337. [CrossRef]
65. Devi, G.N.; Unnisa, C.B.N.; Roopan, S.M.; Hemapriya, V.; Chitra, S.; Chung, I.M.; Kim, S.H.; Prabakaran, M. Floxacins: As Mediators in enhancing the corrosion inhibition efficiency of natural polymer dextrin. *Macromol. Res.* **2020**, *28*, 558–566. [CrossRef]
66. Hemapriya, V.; Chung, I.M.; Parameswari, K.; Chitra, S.; Kim, S.H.; Prabakaran, M. Corrosion inhibition behavior of benzothiazine derivative on low carbon steel in acid medium: Adsorption and quantum chemical investigations. *Surf. Rev. Lett.* **2019**, *26*, 1950066. [CrossRef]
67. Chung, I.M.; Kim, S.H.; Prabakaran, M. Evaluation of phytochemical, polyphenol composition and anti-corrosion capacity of *Cucumis anguria* L. leaf extract on metal surface in sulfuric acid medium. *Prot. Met. Phys. Chem. Surf.* **2020**, *56*, 214–224. [CrossRef]
68. Unnisa, C.B.N.; Chitra, S.; Devi, G.N.; Kiruthika, A.; Roopan, S.M.; Hemapriya, V.; Chung, I.M.; Kim, S.H.; Prabakaran, M. Electrochemical and nonelectrochemical analyses of cardo polyesters at the metal/0.5 M $H_2SO_4$ interface for corrosion protection. *Res. Chem. Intermed.* **2019**, *45*, 5425–5449. [CrossRef]
69. Chung, I.M.; Hemapriya, V.; Kanchana, P.; Arunadevi, N.; Chitra, S.; Kim, S.H.; Prabakaran, M. Active-polyphenolic-compounds-rich green inhibitor for the surface protection of low carbon steel in acidic medium. *Surf. Rev. Lett.* **2020**, *27*, 1950154. [CrossRef]
70. Malathy, R.; Prabakaran, M.; Kalaiselvi, K.; Chung, I.M.; Kim, S.H. Comparative polyphenol composition, antioxidant and anticorrosion properties in various parts of *Panax ginseng* extracted in different solvents. *Appl. Sci.* **2021**, *11*, 93. [CrossRef]
71. Mahalakshmi, D.; Unnisa, C.B.N.; Hemapriya, V.; Subramaniam, E.P.; Roopan, S.M.; Chitra, S.; Chung, I.M.; Kim, S.H.; Prabakaran, M. Anticorrosive potential of ethanol extract of *Delonix elata* for mild steel in 0.5 M $H_2SO_4$—A green approach. *Bulg. Chem. Commun.* **2019**, *51*, 31–37.
72. Manh, T.D.; Huynh, T.L.; Thi, B.V.; Lee, S.; Yi, J.; Dang, N.N. Corrosion inhibition of mild steel in hydrochloric acid environments containing *Sonneratia caseolaris* leaf extract. *ACS Omega* **2022**, *7*, 8874–8886. [CrossRef] [PubMed]